Geochemistry Geophysics Geosystems G3

Article
Volume 11, Number 8
5 August 2010
Q08007, doi:10.1029/2010GC003033
ISSN: 1525-2027

Published by AGU and the Geochemical Society

Variations of the Antarctic Circumpolar Current intensity during the past 500 ka

A. Mazaud, E. Michel, and F. Dewilde

Laboratoire des Sciences du Climat et de l'Environnement, CEA, CNRS, UVSQ, Domaine du CNRS, F-91198 Gif-sur-Yvette, France (alain.mazaud@lsce.ipsl.fr)

J. L. Turon

Environnements et Paléoenvironnements Océaniques, UMR 5805, Université Bordeaux 1, Avenue des Facultés, F-33405 Talence CEDEX, France

[1] We examine the past variations of the Antarctic Circumpolar Current (ACC) by using variations in size and abundance of the magnetic grains deposited by this current at a site east the Kerguelen-Crozet plateau. Core MD00-2375G was taken at a midlatitude site during the ANTAUS cruise conducted in 2000 by the French R/V *Marion Dufresne*. Marine isotope stages (MIS) down to MIS 13 are identified, and an age model is derived from a correlation to the ice core isotopic record obtained from EPICA in Antarctica. Continuous records of abundance and size of the magnetic grains were obtained using environmental magnetism methods. Results show a strong modulation of the ACC flow intensity in response to glacial and interglacial cycles. The low abundance and the small size of magnetic grains indicate that the ACC was weak during warm stages and strong during glacial epochs. A large modulation is also observed at the sub-stage scale during the interglacials. A minimum in concentration and grain size occurs at the onset of MIS 11. At the MIS 6–5, 10–9, and possibly 12–11 transitions, observed variations suggest a mechanism involving both rapid and progressive variations of the ACC flow at deglaciations.

Components: 4200 words, 7 figures.

Keywords: Antarctic; current; past; cycles.

Index Terms: 1512 Geomagnetism and Paleomagnetism: Environmental magnetism; 1635 Global Change: Oceans (1616, 3305, 4215, 4513).

Received 11 January 2010; **Revised** 14 June 2010; **Accepted** 18 June 2010; **Published** 5 August 2010.

Mazaud, A., E. Michel, F. Dewilde, and J. L. Turon (2010), Variations of the Antarctic Circumpolar Current intensity during the past 500 ka, *Geochem. Geophys. Geosyst.*, *11*, Q08007, doi:10.1029/2010GC003033.

1. Introduction

[2] The Southern Ocean has a strong importance in the Earth climatic system, in particular because of the presence of the largest ocean current in the world, the Antarctic Circumpolar Current (ACC). This eastward current flows approximately between 45°S and 55°S and is mainly driven by westerly winds that circle Antarctica. It transports more than 130×10^6 m^3 s^{-1} (Sv) of surface, deep and intermediate waters between the Atlantic, Indian, and Pacific oceans [*Rintoul et al.*, 2001]. ACC therefore plays a crucial role for heat and CO2 balance in the Southern Ocean, and consequently for climate at the

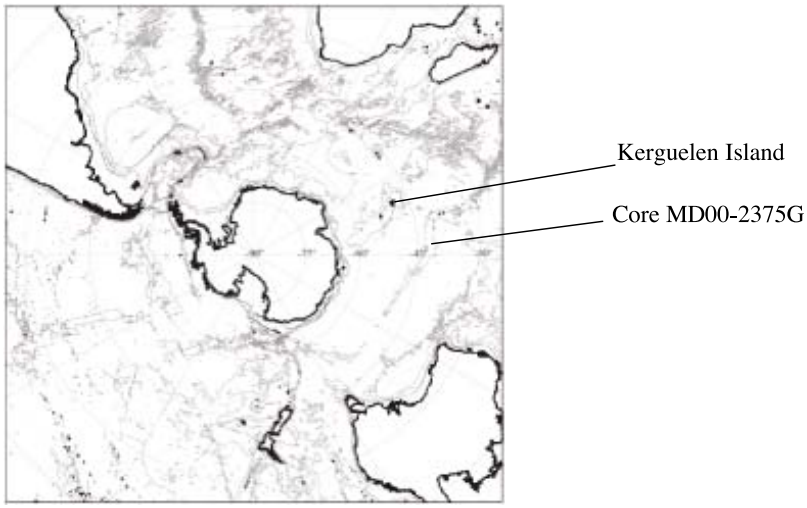

Figure 1. Location of core MD00-2375G in the southern Indian Ocean.

global scale [*Toggweiler et al.*, 2006]. Despite its crucial importance, however, the temporal variations of the ACC during the last climatic cycles and their links with climate evolution are still relatively unknown, in particular in the Kerguelen sector where previous studies focused on the last glacial period and the Holocene [*Dezileau et al.*, 2000]. Here, we present a continuous record of the past variations of the Antarctic Circum Current intensity over the past 500 ka. It is obtained by investigating the size and the abundance of the magnetic grains transported by the ACC from the Kerguelen-Crozet plateau to a site located eastward from this plateau, in the main flow of the ACC.

[3] Core MD00-2375G (45° 42.13′S, 86° 44.26′E, depth: 3485 m) was taken by the French Research Vessel (R,V) *Marion Dufresne* during the ANTAUS cruise in 2000, east of the Kerguelen Plateau, using a gravity coring system. Kerguelen plateau is a large igneous province formed at ~115 Ma from mantle plume activity [*Whitechurch et al.*, 1992], and the Kerguelen archipelago results from flood basalt accumulation since the past 40 Ma [*Nicolaysen et al.*, 2000]. In this area, the ACC flow is deflected by the Kerguelen Plateau and ≈2/3 of the main flow (≈90 Sv) is concentrated within the Sub-Antarctic Front (SAF) north of the Kerguelen Island while 1/3 (≈43 Sv) of the ACC flows through the Fawn trough and then north along the east flank of the Kerguelen Plateau before flowing eastward again [*Park et al.*, 2009] (Figure 2). The studied site (Figures 1 and 2) is located in on oblong sedimentary formation, where material eroded from the Kerguelen and Crozet plateau and transported by the ACC flow accumulates [*Bareille et al.*, 1994; *Dezileau et al.*, 2000]. In the last decade, several marine cores taken in this formation by the R/V *Marion Dufresne* have provided insights on ACC changes during the last climatic cycle. Physical properties and sedimentology have documented a stronger ACC during the last glacial than during the Holocene, with some lateral redistribution [*Dezileau et al.*, 2000]. The Antarctic Bottom Water (AABW) current also flows in this zone, but at a depth deeper than 3600 m at present time, i.e., below the studied site [*Orsi et al.*, 1999]. Northward expansion of AABW may have occurred during the last glacial epoch [*McCave et al.*, 2008; *Govin et al.*, 2009]. However, analyses of rare earths indicate that only a minor amount of particles from Antarctica reached the studied area during the Holocene and the last glacial [*Dezileau et al.*, 2000], suggesting that the AABW transport has a minor contribution at the studied site. Compared to previous piston cores from the same area [*Dezileau et al.*, 2000; *Mazaud et al.*, 2002, 2007], core MD00-2375G covers several climatic cycles and offers opportunity to examine past ACC variations down to marine isotope stage (MIS) 13. Past ACC intensity is studied using environmental magnetism methods, which trace abundance and size of the magnetic grains transported to the site by the ACC flow.

2. Isotopic Record and Age Model

[4] Core MD00-2375G isotopic measurements were obtained on *Globigerina bulloides* specimen from the 250–315 μm range. They where measured at Laboratory of Sciences of Climate and Environnement (LSCE) on an Elementar Isoprime

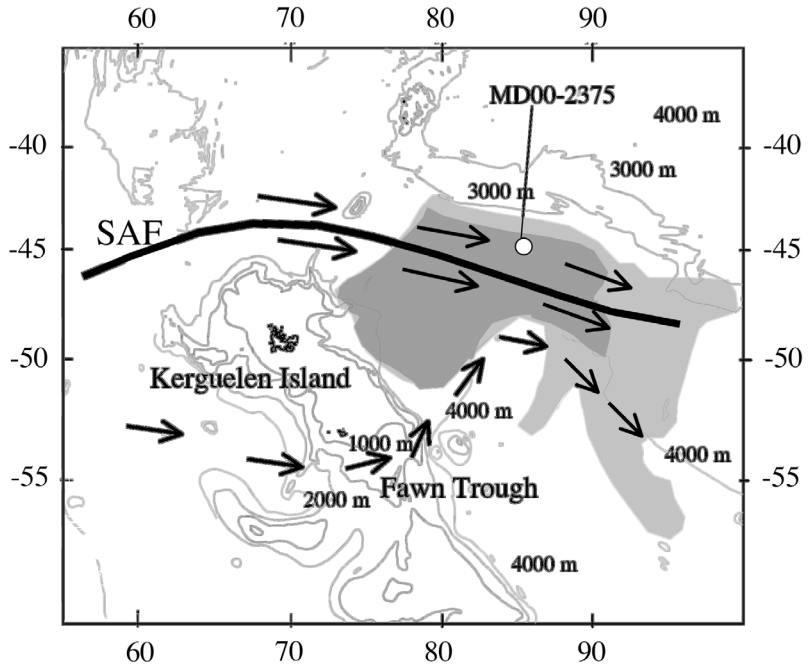

Figure 2. Location of core MD00-2375G in the south Indian Ocean, eastward from the Crozet-Kerguelen Plateau, with regional topography. Gray areas indicate estimates of the sediment thickness, after *Dezileau et al.* [2000], (dark, >250 m, light, <250 m). ACC flow is schematically indicated by arrows.

mass-spectrometers. The $\delta^{18}O$ data are on the Vienna PDB (VPBD) scale defined with respect to the international NBS19 calcite standard. The measured NBS18 $\delta^{18}O$ is -23.2 ± 0.2‰ VPDB and the external reproducibility (1 sigma) of carbonate standards is 0.05‰ for $\delta^{18}O$. The pooled standard deviation calculated from *G. bulloides* replicate measurements on this core is 0.11‰. The age model was derived from a correlation between the $\delta^{18}O$ record of planktonic foraminifera from core MD00-2375G (Figure 3a) and the glaciologic isotopic record obtained from EPICA in Antarctica [*EPICA Community Members*, 2004]. Indeed, major temperature changes occurred quasi-simultaneously in the subantarctic surface waters and in the atmosphere above inland Antarctica [*Sowers et al.*, 1993; *Waelbroeck et al.*, 1995]. Therefore, we tied the $\delta^{18}O$ record of the *G. bulloides* to the deuterium record of EPICA Dome C (EDC) ice core [*EPICA Community Members*, 2004] placed on its most recent time scale EDC3 [*Parrenin et al.*, 2007]. Ages between the tie-points are calculated by a simple linear interpolation (Analyseries software) [*Paillard et al.*, 1996]. A good correspondence is observed between core MD00-2375G isotopic signal and the ice record (Figure 3b). Although such a correlation does not define ages at a millennial precision, isotopic stages down to MIS 13 are clearly identified, which allows discussion of the variations of the ACC at orbital frequencies.

3. Magnetic Methods

[5] Magnetic analyses consist of continuous high-resolution measurements of three bulk magnetic parameters: the volume low-field susceptibility (κ), the anhysteretic remanent magnetization (ARM), and the isothermal remanent magnetization (IRM). κ primarily depends on the amount and nature of ferromagnetic (sensu lato) but also on the presence of paramagnetic and diamagnetic minerals. ARM and IRM, which are remanent magnetizations acquired in laboratory, are solely sensitive to the ferro/ferri magnetic fraction, and do not depend on para/diamagnetic minerals.

[6] κ was measured at the LSCE using a small diameter Bartington coil, allowing a resolution of 4 cm, very close to that of the cryogenic magnetometers used for ARM and IRM determinations. ARM and IRM were measured in the shielded room of the LSCE using high-resolution pass-through 2G cryogenic magnetometers [*Goree and Fuller*, 1976; *Weeks et al.*, 1993] after full demagnetization of the Natural Remanent Magnetization (NRM). ARM was imparted along the axis of the u-channel in a 100 mT AF and 0.05 mT bias field, followed by

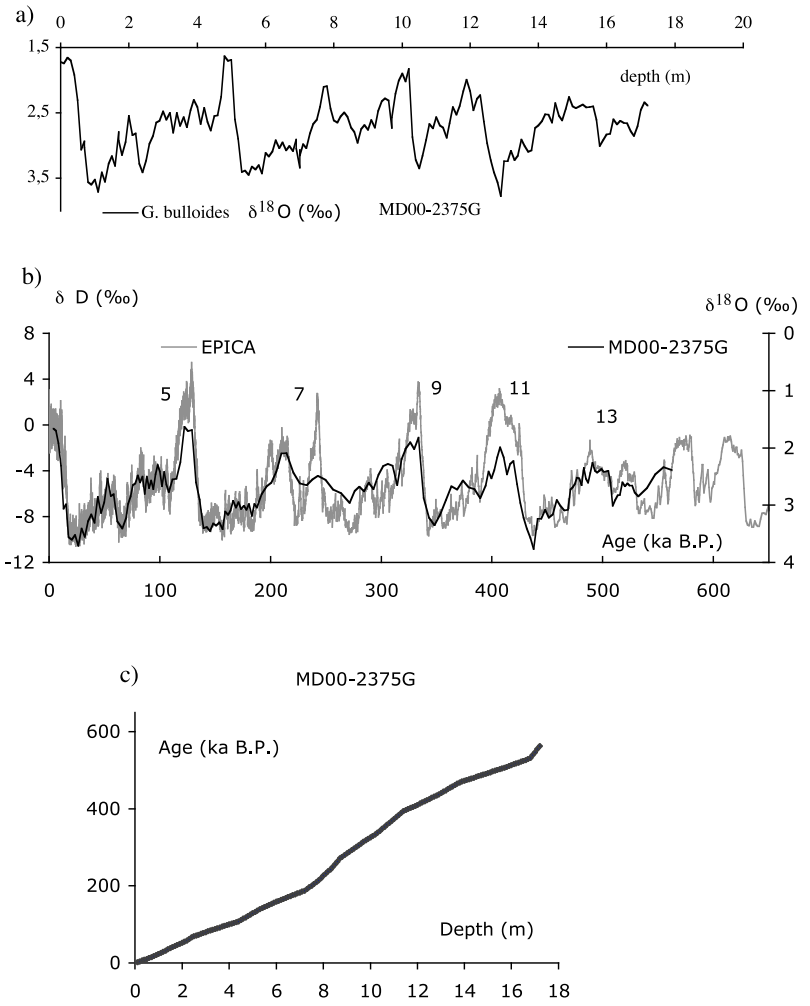

Figure 3. (a) Isotopic record versus depth obtained for core MD00-2375G, (b) correlation with EPICA isotopic temperature record, and (c) obtained age versus depth model.

ARM AF demagnetization with 8 steps from 0 to 70 mT. IRM was then acquired in 6 steps up to 1T using a 2G pulsed IRM solenoid. For these measurements, the core has been continuously subsampled using the u-channel technique [*Tauxe et al.*, 1983; *Weeks et al.*, 1993]. Additional experiments, such as thermomagnetic investigations and determination of the S-ratio, S, which measures the magnetic coercively, were also conducted to examine the magnetic mineralogy downcore. Precisely, S is determined by applying a backfield of 0.3 Tesla (T), after acquisition of the IRM at 1 T ($S = -IRM_{-0.3_T}/IRM1_T$ [*King and Channell*, 1991].

4. Magnetic Grain Deposition During the Past Five Climatic Cycles

[7] ARM versus κ plot shows an elongated dispersion pattern aligned along a single slope (Figure 4a). It indicates variations in magnetic grain concentration downcore with no large change in the magnetic mineralogy [*Banerjee et al.*, 1981]. Homogeneity of the magnetic mineralogy downcore is also indicated by the S-ratio, which does not significantly vary from a value of 0.95 (Figure 4b). It indicates low coercive magnetic minerals, such as low Ti titano-magnetite [*King and Channell*, 1991]. Thermomagnetic investigations (Figure 4c) provide Curie temperatures of 580°C, which characterizes low Ti titano-magnetite. Thus, as for the other cores previously taken in the same sector of the South Indian Ocean [*Mazaud et al.*, 2002, 2007] magnetic mineralogy is dominated by low Ti titano-magnetite with no significant variations downcore.

[8] Thus, we have used environmental magnetism techniques to derive continuous records of past variations of amount and size of the magnetic grains. Indeed, magnetic parameters of sediments

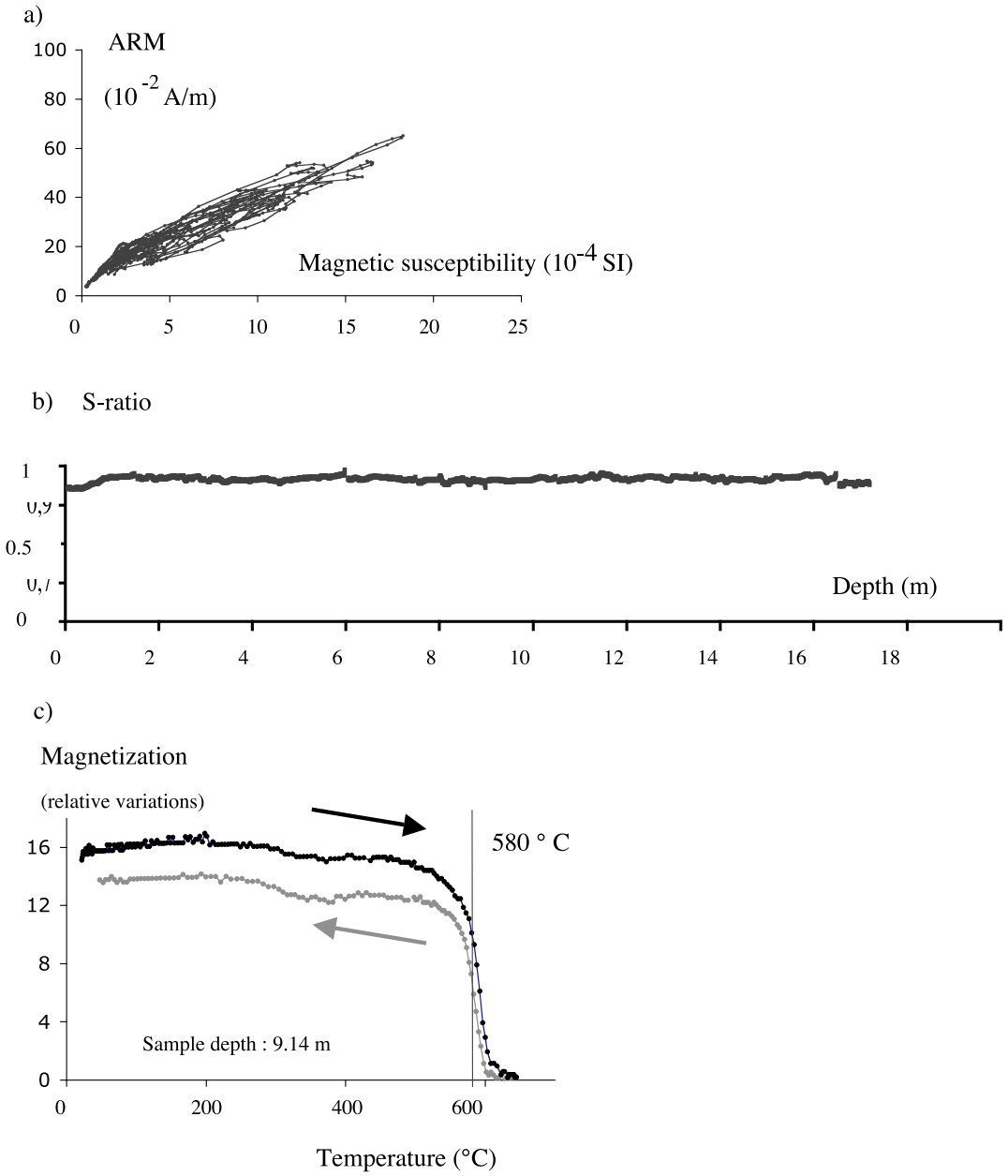

Figure 4. (a) ARM versus κ diagram, (b) S-ratio obtained downcore MD00-2375G, and (c) typical thermomagnetic curve. Arrows indicate cooling and heating.

deposited in a context of a well-defined grain source upstream may be used to trace changes in the intensity of the current which transports the magnetic grains [*Kissel et al.*, 1999, 2009].

4.1. Concentration Changes

[9] The 3 bulk magnetic parameters consistently exhibit values larger during cold MIS than during interglacials (Figure 5). Because of the homogeneous magnetic mineralogy downcore, these glacial-interglacial variations indicate changes in concentration of magnetite and not changes in mineralogy. Close similarity also indicates negligible contribution of paramagnetic minerals, such as clay, because paramagnetism affects κ but not IRM and ARM. Figure 5 shows a modulation during stages 5 and 7, with lower concentrations during warm substages than during cold sub-stages. Bulk magnetic parameters also indicate a minimal concentration of magnetite at the onset of MIS11 (Figure 5).

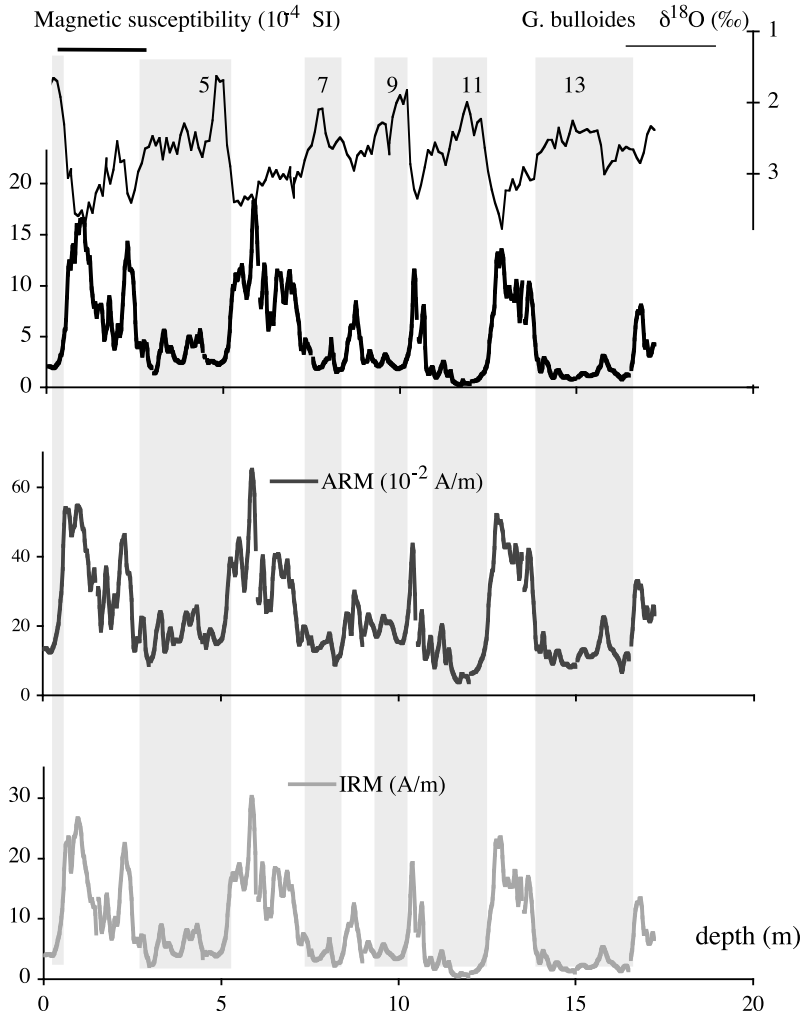

Figure 5. The κ, ARM, IRM records obtained for core MD00-2375G. The isotopic record of Figure 3a is also reported if Figure 5 (top). Marine isotopic stages, identified by the correlation to the EPICA glaciologic isotopic record, are indicated.

[10] Lower concentration of magnetite during warm MISs than during cold MISs may reflect variations in the deposition rate of magnetite by the ACC, but also variations in the dilution by non-magnetic materials. To investigate this point, we have calculated a flux of magnetite, using core MD00-2375G age model. A value of 5 10^{-4} m^3 kg^{-1} was used for the specific mass susceptibility of magnetite [*Thompson and Oldfield*, 1986], in order to calculate masses of magnetite deposited per surface unit and per ka (g/cm^2/ka). The calculated flux versus age strongly resembles the low field susceptibility bulk record (Figure 6). The magnetite flux is lower during interglacials than during glacial periods. During MIS 5, the modulation observed in the bulk magnetic records is still visible (Figure 6). Thus, bulk magnetic parameters principally trace temporal changes in the flux of magnetite deposited by the ACC at site MD00-2375G, and not a variable dilution by other materials.

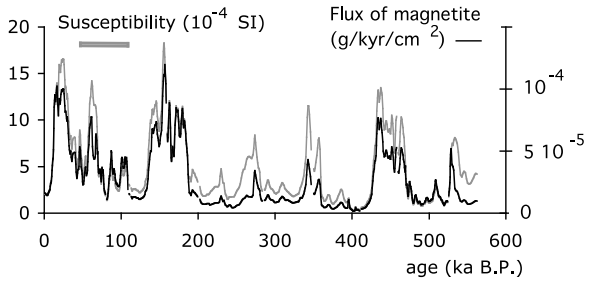

Figure 6. Flux of magnetite obtained versus age (dark curve, see text for explanations). Initial low field susceptibility, κ, is also reported (gray curve).

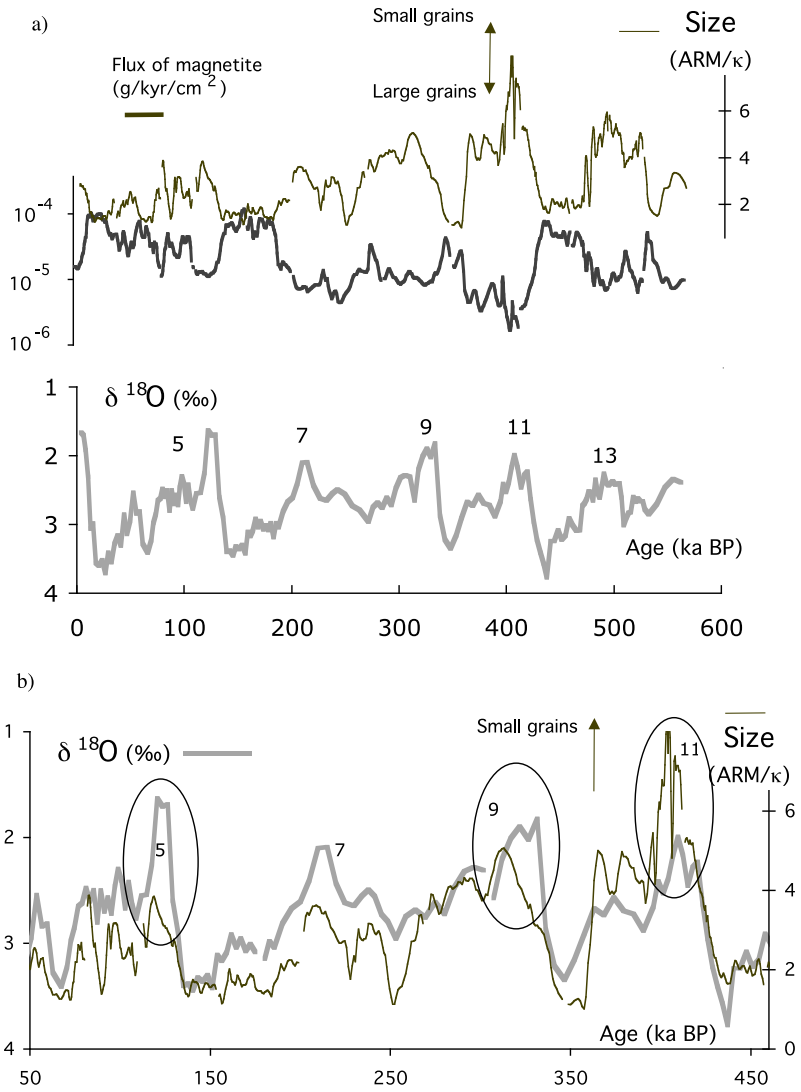

Figure 7. (a) Flux of magnetite versus age (thick line, same as Figure 6 but with a log. scale) together with magnetic grain size variations as seen by ARM/κ (thin line, relative variations). Isotopic record is also shown. (b) Zoom of isotopic and grain size records for stages 5 to 11 (encircled zones are discussed in more detail in the text).

4.2. Magnetic Grain Size Changes

[11] The κ, ARM, and IRM are also dependent on magnetic grain size. For magnetite, ARM is sensitive to small grains, with size around 0.1–5 μm, while IRM and κ are both sensitive to a larger range of sizes [*Maher*, 1988; *Dunlop and Özdemir*, 1997]. Consequently, differences between ARM and κ (or between ARM and IRM) can be used to trace grain size variations when the magnetic mineralogy does not significantly vary downcore. For low Ti titano-magnetite, ARM/κ is classically used to trace grain size variations [*Maher*, 1988; *Dunlop and Özdemir*, 1997]. Low values of ARM/κ indicate large grains, while large values correspond to small grains.

[12] The smallest grains were deposited during the interglacials, when the magnetite flux was also low (Figure 7a). During MIS 5, the smallest grains were deposited during warm sub-stages 5a, 5c, and 5e. A modulation is also observed during MIS 7 (Figure 7a). For the entire core, the smallest magnetite grains are found at the onset of stage 11, when the concentration in magnetite is also minimal (Figure 7a). This coincidence between grain size variations and concentration changes indicates that the efficiency of the ACC flow to convey magnetite grains to MD00-2375G site was stronger during cold periods

(large abundance of magnetite with large grains) than during warm epochs (low amount of magnetite and small grains).

5. Implications for the ACC Variation

[13] Changes in magnetite grain transport may indicate reinforcements of the ACC flow intensity during cold periods, but also latitudinal changes of the main ACC flow, with a northward displacement during glacial epochs associated to shifts of the fronts systems [*Howard and Prell*, 1992], especially the SAF which dominates the transport of the ACC. However, several cores distributed at different latitudes in the same sector consistently reveal a stronger deposition by the ACC during the last Glacial than during the Holocene [*Dezileau et al.*, 2000]. As changes in ACC latitude would have affected differently cores at different latitudes, it is likely that the variations observed at site MD00-2375G principally trace a modulation of ACC intensity. Correlation between magnetic susceptibility of marine cores under the ACC and Antarctic ice cores dust has been observed, initially by *Petit et al.* [1990], and more recently by *Pugh et al.* [2009]. Geochemical analyses demonstrated the Aeolian dust deposited during glacial epochs in eastern Antarctic ice mostly originates from South America [*Grousset et al.*, 1992; *Gaiero*, 2007]. However, the direct input of Aeolian dust in sediments east of the Kerguelen Plateau is negligible, or very minor [*Bareille et al.*, 1994]. Thus, observed variations in magnetite amount and grain size do not reflect direct aeolian input but change in ACC flow speed. Past ACC changes observed at the glacial-interglacial scale were mainly driven by wind stress changes [*Bareille et al.*, 1994; *Dezileau et al.*, 2000; *Pugh et al.*, 2009], as for dust deposited over Antarctica. Various studies have attempted to estimate the possible increase of the westerlies intensity and/or their latitudinal migration in the past (see *Shulmeister et al.* [2004] and *Moreno et al.* [2009] for reviews). While these studies do not extend further than the last glacial period, our data support previous evidence that westerlies intensity was higher during the last glacial maximum [*Shulmeister et al.* 2004]. Further, it indicates that the westerlies intensity, recorded here through the ACC flow, was also higher during previous glacial periods and has been modulated over glacial-interglacial periods.

[14] On a shorter time scales, a modulation of amount and size of magnetite grains is visible, in particular during the interglacials. It suggests a strongly reduced ACC speed during the warmest sub-stages, with a marked minimum corresponding to MIS11.

[15] We examine now in more detail changes in magnetic grain size at the transition 6–5. At the end of MIS6, grain size decrease and $\delta^{18}O$ decrease started simultaneously (Figure 7b, encircled zone). Then, the rate in grain size change slowed down during the $\delta^{18}O$ plateau of the interglacial. Grain size minimum occurred at the end of MIS 5e (Figure 7b, encircled zone). The age model suggests a value of about 6 ka for this lag. A similar phasing is also observed at the MIS10–9 transition (Figure 7b), with an estimated lag of about 15 ka. Although less visible, a similar scenario may have occurred at the MIS12–11 transition (Figure 7b, encircled zone).

[16] The initial reduction of grain size synchronous with planktonic $\delta^{18}O$ changes suggests a rapid ACC flow change at deglaciations. Then, the decrease in grain size observed while the $\delta^{18}O$ slope does not change suggests a further delayed response of the ACC.

6. Conclusion

[17] Concomitant variations in the magnetite flux and in magnetic grain size at site MD00-2375G indicate alternate periods of strong and weak deposition of magnetic grains by the ACC flow, in connection with the climatic cycles. It confirms and extends over the past 5 climatic cycles the scheme of a variable wind stress control of ACC flow closely connected with the alternation of glacial and interglacial periods. Variations observed on shorter time scale at the MIS 6–5, 10–9, and possibly 12–11 transitions, suggest a mechanism involving both rapid and progressive variations of the ACC flow. Further studies at different latitudes in the same sector will be needed to better investigate the different mechanisms involved and their evolution through time.

Acknowledgments

[18] We thank the French institute IPEV, the crew of the R/V *Marion Dufresne* and Yvon Balut, the chief of the operations. We also thank Louis Géli, the chief of the ANTAUS cruise. We are most grateful to the two anonymous reviewers for their constructive comments that helped to improve greatly the manuscript. This study has been funded by the French Commissariat à l'Energie Atomique, the Centre National de la Recherche Scientifique and by the French ANR PICC 05-BLAN-0312-01. LSCE contribution 4253.

References

Banerjee, S. K., J. King, and J. Marvin (1981), A rapid method for magnetic granulometry with applications to environmental studies, *Geophys. Res. Lett.*, *8*(4), 333–336, doi:10.1029/GL008i004p00333.

Bareille, G., F. Grousset, M. Labracherie, L. Labeyrie, and J. R. Petit (1994), Origin of detrital fluxes in the southeast Indian Ocean during the last climatic cycles, *Paleoceanography*, *9*, 799–819, doi:10.1029/94PA01946.

Dezileau, L., G. Bareille, J. L. Reyss, and F. Lemoine (2000), Evidence for strong sediment redistribution by bottom currents along the southeast Indian ridge, *Deep Sea Res., Part I*, *47*(10), 1899–1936, doi:10.1016/S0967-0637(00)00008-X.

Dunlop, D., and Ö. Özdemir (1997), *Rock Magnetism: Fundamentals and Frontiers*, *Cambridge Stud. Magnet*, vol. 3, 595 pp., Cambridge Univ. Press, Cambridge, U. K.

EPICA Community Members (2004), Eight glacial cycles from an Antarctic ice core, *Nature*, *429*, 623–628, doi:10.1038/nature02599.

Gaiero, D. M. (2007), Dust provenance in Antarctic during glacial periods from where in southern South America, *Geophys. Res. Lett.*, *34*, L17707, doi:10.1029/2007GL030520.

Goree, W. S., and M. Fuller (1976), Magnetometers using R.F. driven squids and their applications in rock magnetism and paleomagnetism, *Rev. Geophys. Space Phys.*, *14*, 591–608, doi:10.1029/RG014i004p00591.

Govin, A., E. Michel, L. Labeyrie, C. Waelbroeck, F. Dewilde, and E. Jansen (2009), Evidence for northward expansion of Antarctic Bottom Water mass in the Southern Ocean during the last glacial inception, *Paleoceanography*, *24*, PA1202, doi:10.1029/2008PA001603.

Grousset, F. E., P. E. Biscaye, M. Revel, J. R. Petit, K. Pye, S. Joussaume, and J. Jouzel (1992), Antarctic (Dome C) ice-core dust at 18 k.y. B.P.: Isotopic constraints on origin and atmospheric circulation, *Earth Planet. Sci. Lett.*, *111*, 175–182, doi:10.1016/0012-821X(92)90177-W.

Howard, W. R., and W. L. Prell (1992), Late Quaternary surface circulation of the southern Indian Ocean and its relationship to orbital variations, *Paleoceanography*, *7*, 79–117, doi:10.1029/91PA02994.

King, J. W., and J. E. T. Channell (1991), Sedimentary magnetism, environmental magnetism, and magnetostratigraphy, *U.S. Natl. Rep. Int. Union Geod. Geophys. 1987–1990*, *Rev. Geophys.*, *29*, suppl., 358–370.

Kissel, C., C. Laj, L. Labeyrie, T. Dokken, A. Voelker, and D. Blamart (1999), Rapid climatic variations during marine isotopic stage 3: Magnetic analysis of sediments from Nordic Seas and North Atlantic, *Earth Planet. Sci. Lett.*, *171*, 489–502, doi:10.1016/S0012-821X(99)00162-4.

Kissel, C., C. Laj, T. Mulder, C. Wandres, and M. Cremer (2009), The magnetic fraction: A tracer of deep water circulation in the North Atlantic, *Earth Planet. Sci. Lett.*, *288*, 444–454, doi:10.1016/j.epsl.2009.10.005.

Maher, B. A. (1988), Magnetic-properties of some synthetic sub-micron magnetites, *Geophys. J.*, *94*(1), 83–96.

Mazaud, A., M. A. Sicre, U. Ezat, J. J. Pichon, J. Duprat, C. Laj, C. Kissel, L. Beaufort, E. Michel, and J. L. Turon (2002), Geomagnetic-assisted stratigraphy and sea-surface temperature changes in core MD94-103(southern Indian Ocean): Possible implications for north-south climatic relationship around H4, *Earth Planet. Sci. Lett.*, *201*, 159–170, doi:10.1016/S0012-821X(02)00662-3.

Mazaud, A., C. Kissel, C. Laj, M. A. Sicre, E. Michel, and J. L. Turon (2007), Variations of the ACC-CDW during MIS3 traced by magnetic grain deposition in midlatitude south Indian Ocean cores: Connections with the Northern Hemisphere and with central Antarctica, *Geochem. Geophys. Geosyst.*, *8*, Q05012, doi:10.1029/2006GC001532.

McCave, I. N., L. Carter, and I. R. Hall (2008), Glacial-interglacial changes in water mass structure and flow in the SW Pacific Ocean, *Quat. Sci. Rev.*, *27*, 1886–1908, doi:10.1016/j.quascirev.2008.07.010.

Moreno, P. I., J. P. François, R. P. Villa-Martinez, and C. M. Moy (2009), Millennial-scale variability in Southern Hemisphere westerly wind activity over the last 5000 years in SW Patagonia, *Quat. Sci. Rev.*, *28*, 25–38, doi:10.1016/j.quascirev.2008.10.009.

Nicolaysen, K., F. A. Frey, K. V. Hodges, D. Weis, and A. Giret (2000), $^{40}Ar/^{39}Ar$ geochronology of flood basalts from the Kerguelen Archipelago, southern Indian Ocean: Implications for Cenozoic eruption rates of the Kerguelen plume, *Earth Planet. Sci. Lett.*, *174*, 313–328, doi:10.1016/S0012-821X(99)00271-X.

Orsi, A. H., G. C. Johnson, and J. L. Bullister (1999), Circulation, mixing, and production of Antarctic Bottom Water, *Prog. Oceanogr.*, *43*, 55–109, doi:10.1016/S0079-6611(99)00004-X.

Paillard, D., L. Labeyrie, and P. Yiou (1996), Macintosh program performs time-series analysis, *Eos Trans. AGU*, *77*, 379, doi:10.1029/96EO00259.

Park, Y. H., F. Vivier, F. Roquet, and E. Kestenare (2009), Direct observations of the ACC transport across the Kerguelen Plateau, *Geophys. Res. Lett.*, *36*, L18603, doi:10.1029/2009GL039617.

Parrenin, F., et al. (2007), The ECD3 chronology for the EPICA Dome C ice core, *Clim. Past*, *3*, 485–497, doi:10.5194/cp-3-485-2007.

Petit, J. R., L. Mounier, J. Jouzel, Y. S. Korokevich, V. I. I. Kotlyakov, and C. Lorius (1990), Paleoclimatological and chronological implications of the Vostok core dust record, *Nature*, *343*, 56–58, doi:10.1038/343056a0.

Pugh, R. S., I. N. McCave, C.-D. Hillenbrand, and G. Kuhn (2009), Circum-Antarctic age modelling of Quaternary marine cores under the Antarctic Circumpolar Current: Ice-core dust-magnetic correlation, *Earth Planet. Sci. Lett.*, *284*(1–2), 113–123, doi:10.1016/j.epsl.2009.04.016.

Rintoul, S. R., C. Hughes, and D. Olbers (2001), The Antarctic Circumpolar Current system, in *Ocean Circulation and Climate: Observing and Modelling the Global Ocean*, edited by G. Siedler, J. Church, and J. Gould, pp. 271–301, Academic, San Diego, Calif.

Shulmeister, J., et al. (2004), The Southern Hemisphere westerlies in the Australasian sector over the last glacial cycle: A synthesis, *Quat. Int.*, *118–119*, 23–53, doi:10.1016/S1040-6182(03)00129-0.

Sowers, T., M. Bender, L. Labeyrie, D. Martinson, J. Jouzel, D. Raynaud, J. J. Pichon, and Y. S. Korotkevich (1993), A 135,000-year Vostok-Specmap common temporal framework, *Paleoceanography*, *8*, 737–766, doi:10.1029/93PA02328.

Tauxe, L., J. L. La Brecque, R. Dodson, M. Fuller, and J. Dematteo (1983), 'U' channels—A new technique for paleomagnetic analysis of hydraulic piston cores, *Eos Trans. AGU*, *64*, 219.

Thompson, R., and F. Oldfield (1986), *Environmental Magnetism*, 227 pp., Allen and Unwin, London.

Toggweiler, J. R., J. L. Russell, and S. R. Carson (2006), Midlatitude westerlies, atmospheric CO_2, and climate change

during the ice ages, *Paleoceanography*, *21*, PA2005, doi:10.1029/2005PA001154.

Waelbroeck, C., J. Jouzel, L. Labeyrie, C. Lorius, M. Labracherie, M. Stievenard, and N. I. Barkov (1995), A comparison of the Vostok ice deuterium record and series from the Southern Ocean core MD88-770 over the last two glacial-interglacial cycles, *Clim. Dyn.*, *12*, 113–123, doi:10.1007/BF00223724.

Weeks, R. J., C. Laj, L. Endignoux, M. Fuller, A. P. Roberts, R. Manganne, E. Blanchard, and W. Goree (1993), Improvements in long-core measurements techniques: Applications in paleomagnetism and palaeoceanography, *Geophys. J. Int.*, *114*, 651–662, doi:10.1111/j.1365-246X.1993.tb06994.x.

Whitechurch, H., R. Montigny, J. H. Sevigny, M. Storey, and V. Salters (1992), K-Ar and $^{40}Ar/^{39}Ar$ ages of central Kerguelen Plateau basalts, *Proc. Ocean Drill. Program Sci. Results*, *120*, 71–77.